ISSN 1392–1320 MATERIALS SCIENCE (MEDŽIAGOTYRA). Vol. 19, No. 1. 2013

Friction Characteristics of Nitrided Layers on AISI 430 Ferritic Stainless Steel Obtained by Various Nitriding Processes

Hakan AYDIN [1] *, Ali BAYRAM [1], Şükrü TOPÇU [2]

[1] *Department of Mechanical Engineering, Faculty of Engineering and Architecture, Uludağ University, 16059, Görükle-Bursa, Turkey.*
[2] *Mgi Coutier, NOSAB, 16140, Nilüfer-Bursa, Turkey.*

crossref http://dx.doi.org/10.5755/j01.ms.19.1.3819

Received 28 November 2011; accepted 28 May 2012

The influence of plasma, gas and salt-bath nitriding techniques on the friction coefficient of AISI 430 ferritic stainless steel was studied in this paper. Samples were plasma nitrided in 80 % N_2 + 20 % H_2 atmosphere at 450 °C and 520 °C for 8 h at a pressure of 2 mbar, gas nitrided in NH_3 and CO_2 atmosphere at 570 °C for 13 h and salt-bath nitrided in a cyanide-cyanate salt-bath at 570 °C for 1.5 h. Characterisation of nitrided layers on the ferritic stainless steel was carried out by means of microstructure, microhardness, surface roughness and friction coefficient measurements. Friction characteristics of the nitrided layers on the 430 steel were investigated using a ball-on-disc friction-wear tester with a WC-Co ball as the counter-body under dry sliding conditions. Analysis of wear tracks was carried out by scanning electron microscopy. Maximum hardness and maximum case depth were achieved on the plasma nitrided sample at 520 ºC for 8 h. The plasma and salt-bath nitriding techniques significantly decreased the average surface roughness of the 430 ferritic stainless steel. The friction test results showed that the salt-bath nitrided layer had better friction-reducing ability than the other nitrided layers under dry sliding conditions. Furthermore, the friction characteristic of the plasma nitrided layer at 520 ºC was better than that of the plasma nitrided layer at 450 °C.

Keywords: 430 ferritic stainless steel, plasma nitriding, salt-bath nitriding, gas nitriding; microhardness; dry sliding friction; friction coefficient.

1. INTRODUCTION

Stainless steels are widely used in the chemical, food, and other industries due to its corrosion-resistant properties [1]. However, low hardness and poor wear resistance sometimes limit its industrial applications. One of the principal methods of improving workpiece performance in the metal-mechanical industry is to achieve a decrease in friction coefficient and thus an increase in wear resistance [2]. Surface engineering is an optional process to improve the surface friction characteristics of stainless steels.

Among many surface engineering techniques, plasma nitriding is the most successfully and widely used technique to engineer the surfaces of stainless steels. Nitriding is a thermochemical surface treatment used in steels and alloys to improve wear and friction properties by surface microstructure modification while maintaining adequate substrate properties [2, 3]. It is a thermochemical process involving the diffusion of atomic nitrogen into the surface of target materials to form hard nitrides of the metal elements constituting the steel. For example, nitriding of stainless steels at a temperature above 500 °C can significantly improve the surface hardness and wear properties [4]. It is well known that plasma nitriding offers many advantages over traditional gas nitriding and salt-bath nitriding, particularly in terms of reduced gas consumption, reduced energy consumption, and the removal of environmental hazards [5, 6]. In addition, during the plasma nitriding process, the sputtering effect of energetic positive ions can effectively remove the oxide film (Cr_2O_3) on the surface and thus accelerate nitrogen mass transfer. Accordingly, plasma nitriding can be carried out in a wider range of temperatures and at a faster nitriding rate than the conventional gaseous and salt bath nitriding processes [1, 7, 8]. However, an increase in surface hardness is often accompanied by a decrease in corrosion properties due to precipitating CrN, especially in the traditional plasma nitriding used widely in industry production [9]. Many attempts have thus been made in the past decade to improve the corrosion resistance of nitrided stainless steels. As a result of these attempts, it has been found that at low temperatures, plasma nitriding can produce a thin layer that has completely different structures and properties than that produced at high temperatures. It has recently been established that the low temperature nitrided layer has a high hardness and excellent corrosion resistance [7, 10 – 12].

Ferritic stainless steels that form a kind of stainless steel are basically iron–chromium alloys with sufficient chromium and other elements, such as Mo, Si, and Al, to stabilise the ferrite phase with a body centred cubic (b.c.c.) structure at all temperatures [13 – 16]. They are not frequently used in conditions requiring resistance to wear because they are softer relative to the other stainless steel grades. However, as mentioned above, wear-resistant stainless steels can be obtained by various surface modifications. In the past few decades, the plasma nitriding technique has been widely used by several authors [1, 4, 5, 7, 9, 17 – 21] to improve the surface performance, such as hardness, wear and corrosion resistance, of austenitic and martensitic stainless steels.

*Corresponding author. Tel.: +90-224-2940652; fax.: +90-224-3941903.
E-mail address: *hakanay@uludag.edu.tr* (H. Aydin)

However, no published results appear for plasma nitrided AISI 430 ferritic stainless steels, and a comparative study on the friction characteristics of plasma, gas and salt-bath nitrided 430 ferritic stainless steels has not been conducted so far. The friction characteristic can be a key property of performance for various applications of ferritic stainless steels. Therefore, the aim of the present investigation is a comparative study on the friction characteristics of plasma, gas and salt-bath nitrided 430 ferritic stainless steels using a ball-on-disc friction-wear tester with a WC-Co ball as the counterface under dry sliding conditions. The surface roughnesses, microstructures and microhardness profiles of the nitrided layers were also examined.

2. EXPERIMENTAL PROCEDURE

2.1. Materials

The alloy studied here (AISI 430 ferritic stainless steel) has the following composition (wt.%): C, 0.055; Si, 0.352; Mn, 0.302; P, 0.023; S, 0.011; Cr, 15.76; Mo, 0.085; Ni, 0.419; Al, 0.0052; Co, 0.036; Cu, 0.143; Nb, 0.044; V, 0.078; W, 0.049; and Fe, balance. Samples of 15-mm-thick 430 ferritic stainless steel were cut from bars that were 25.4 mm in diameter. The discs were first ground on a grinding machine using a SiC grinding wheel rotating at 800 rpm and finally cleaned with acetone in an ultrasonic cleaner prior to the nitriding processes.

2.2. Nitriding processes

The disc samples have been nitrided using the plasma, gas and salt-bath nitriding techniques. Before the plasma nitriding step, sputter cleaning was performed in a high-density pure hydrogen atmosphere at about 430 °C for 45 min, which removed the oxide layers formed on the surface of the samples. Then, the 430 ferritic stainless steel samples were plasma nitrided on a PP 60 kW Plateg commercial plasma-nitriding unit with 60-A pulse plasma generator at 450 °C and 520 °C for a total duration of 8 h in a gas mixture of 80 % N_2 + 20 % H_2 at 2 mbar. Fig. 1 shows a schematic of the plasma nitriding system used in this work [22].

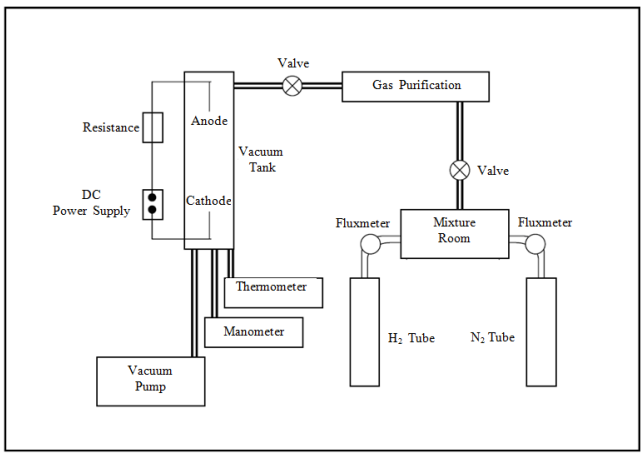

Fig. 1. Scheme of the plasma nitriding system used in this work [22]

Upon the completion of the plasma nitriding processes, the samples were slowly cooled in the chamber to room temperature under flowing nitrogen to protect the surface from oxidation.

The salt-bath nitriding process of the 430 samples was carried out in a cyanide-cyanate salt bath at 570 °C for 1.5 h followed by pre-heating at 325 °C for 1 hour. Then, the samples were cooled in the air to room temperature. Gas nitriding was conducted on an electrical resistance furnace (IPSAN CRV 400 trade mark) in vacuum using a NH_3 and CO_2 atmosphere at 570 °C for 13 h. After the completion of the gas nitriding operation, samples were cooled in the furnace to 30ºC under flowing nitrogen.

2.3. Microstructure analyses and microhardness and surface roughness measurements

The cross-sectioned samples were used to examine the microstructure of the nitrided layers formed on the 430 ferritic stainless steel with an optical microscope after Nital 4 % etching. The case depth of the nitrided layers was determined from optical images. The morphologies of the wear tracks was also investigated using a scanning electron microscope (SEM). Changes in the mechanical properties of the nitrided surfaces of the samples were characterised by microhardness tests. The microhardness tests were performed on a Vickers microhardness tester with a load of 10 g and a dwell time of 15 s by taking five readings to determine the average values. The microhardness depth profile was determined by taking the microhardness measurements from the edge towards the core of the cross-sectioned samples. In addition, because the surface roughness is an important factor for friction characteristics, the surface roughness of the nitrided surfaces was measured by a TR200 Roughness Tester that had a tracking length of 5 mm and least count of 0.001 μm. It measured the average roughness (R_a) over the entire sample.

2.4. Friction testing

A series of experiments were carried out to study the influence of plasma, salt-bath and gas nitriding techniques on the friction characteristics of 430 ferritic stainless steel. Friction characteristics of the nitrided samples were evaluated on a friction-wear tester without lubrication at room temperature in a ball-on-disc contact configuration with friction data collection and display capabilities [23]. The friction coefficient was automatically recorded with a charter connected to the test rig. During tests, the samples (discs) were rotated against a stationary WC/Co ball of 5 mm in diameter at a speed of 8.6 mm/s under dry sliding conditions. The nominal diameter of the wear track was 9 mm, and the normal contact load was 4.1 N. The sliding distance was 68 m for all nitrided samples. The relative humidity of the environment was kept constant between 35 % and 40 % during the friction tests.

3. RESULTS AND DISCUSSION

3.1. Microstructure

Plasma nitriding, salt-bath nitriding and gas nitriding techniques produced different nitride layers in the 430 ferritic stainless steel surfaces in terms of morphology and

thickness. The cross-sectional micrographs of the 450 °C and 520 °C plasma, salt-bath and gas nitrided 430 samples can be seen in Fig. 2.

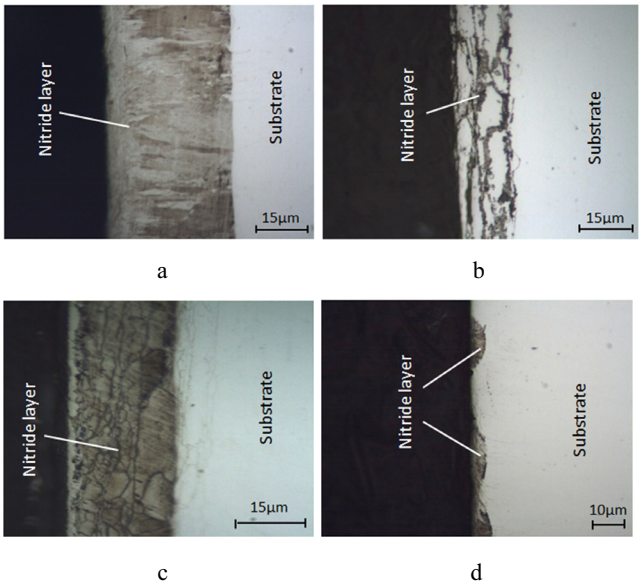

Fig. 2. Optical images of: (a) 520 °C plasma, (b) 450 °C plasma, (c) salt-bath and (d) gas nitrided 430 ferritic stainless steels

The treated layers are clearly visible. According to the pictures, the modified layers of the 430 ferritic stainless steel appear in the samples after etching, with each layer separated from the matrix by a strongly etched line. Fig. 2 shows that a well-defined planar interface between the diffusion zone and the substrate was developed; this behaviour was verified for the plasma nitriding, especially at 520 °C, and salt-bath nitriding techniques. This morphology is due to the distinction in the crystal structures between the nitrided layer and substrate. The case depths of the 450 °C and 520 °C plasma nitrided as well as salt-bath nitrided layers of 430 samples were measured to be about 28 µm, 64 µm and 38 µm, respectively. The maximum case depth was observed on the plasma nitrided samples at 520 °C. As expected, plasma nitriding at 520 °C produced a thicker nitride layer than plasma nitriding at 450 °C. However, there was no obvious or homogeneous nitride layer on the gas nitrided samples. The nitride layer formed on the gas nitrided sample was in local and preferential regions as well as very thin (Fig. 2, d), which means that the gas nitriding procedure at 570 °C for 13 h was not sufficient to form a hard nitride layer on the 430 ferritic stainless steel surfaces.

The metallographic analysis showed that the salt-bath nitriding process produced a relatively thick nitrided layer consisting of a white layer with a thickness of approximately 2 µm – 3 µm at the top and an adjacent nitrogen diffusion layer on the 430 ferritic stainless steel surfaces (Fig. 2, c). The white layer is resistant to corrosion by the etchant Nital 4 %, and thus it appears to be bright under optical microscopy. The white layer consists of extremely hard iron nitrides [24 – 26], and it has very hard profile but so brittle that it may spall in use [27]. On the other hand, the plasma nitrided layers on the 430 steel surfaces consist of only the nitrogen diffusion layer (Fig. 2, a and b). The 520 °C plasma nitriding process of ferritic stainless steels produced a thicker layer, which is predominantly "dark" in appearance after etching with some "white" phases, characterised by the effective precipitation of chromium nitride, whilst the dark particles were observed in the diffusion layer of the 450 °C plasma nitrided sample along the grain boundaries due to the precipitation of chromium nitrides [7, 28].

3.2. Surface roughness and microhardness

The surface roughness is an important factor for the friction characteristics of nitrided samples. The average surface roughness (R_a) values of the nitrided samples can be seen in Fig. 3.

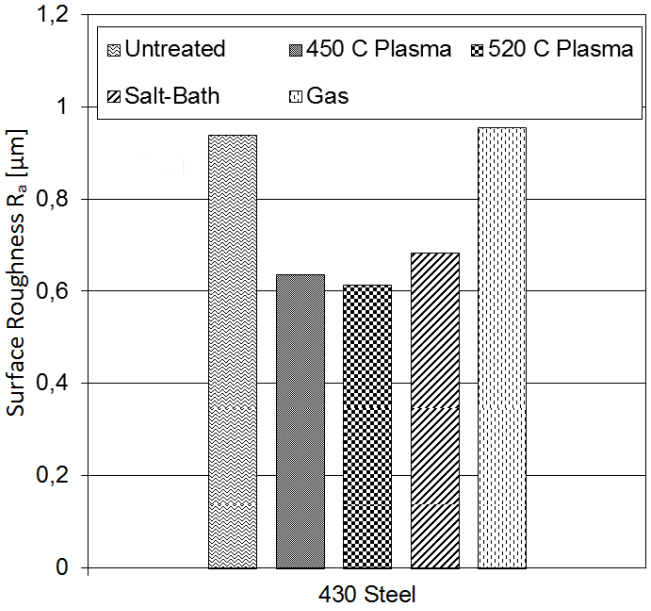

Fig. 3. Surface roughness of the untreated and nitrided 430 ferritic stainless steel samples

The plasma and salt-bath nitriding techniques significantly decreased the average surface roughness of the 430 ferritic stainless steel samples. The surface roughness values of the plasma nitrided and salt-bath nitrided samples are similar. The lowest average surface roughness value was measured to be about 0.613 µm in the 520 °C plasma nitrided sample, whilst the highest surface roughness for the nitrided 430 samples was observed with the gas nitriding procedure. The surface roughness value of the gas nitrided samples is close to that of the untreated samples because the gas nitriding process at 570 °C for 13 h was not sufficient to form an obvious and homogeneous nitrided layer.

The microhardness was measured along the depth on the cross section of the nitrided samples. The hardness profiles in Fig. 4 show a strong hardening effect with the plasma and salt-bath nitriding. The characteristic maximum surface hardness in the plasma and salt-bath nitrided 430 steel samples drops abruptly at the case/core interface to the substrate microhardness value. This is associated with the nitrogen compositional profile through the nitrided surface, developed as a consequence of the nitriding mechanism [2, 29].

As shown in Fig. 4, the microhardness of the substrate was measured as (235 – 245) $HV_{0.01}$, whereas those of the plasma and salt-bath nitrided layers were approximately (1300 – 1500) $HV_{0.01}$.

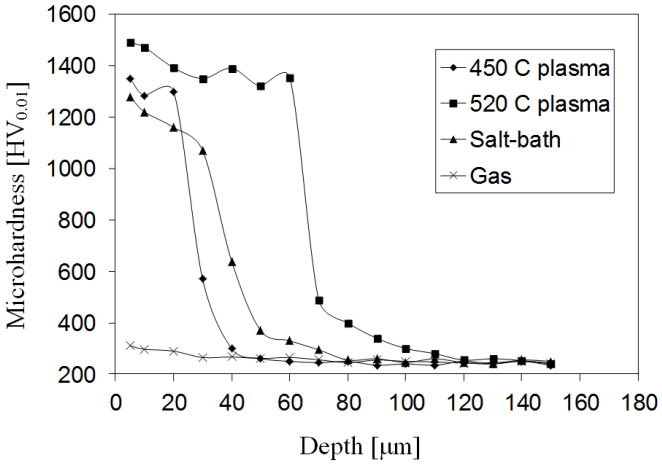

Fig. 4. Microhardness profiles measured along depth on the cross-section of the plasma, salt-bath and gas nitrided nitrided 430 ferritic stainless steel samples

The maximum hardness value measured from the 520 ºC plasma nitrided surface was observed to be 1490 $HV_{0.01}$, which is about 6.3 times as hard as the untreated material. This dramatic increase in surface hardness was due to a fine and homogeneous coherent chromium nitride precipitation of CrN type [2, 30]. As discussed in the literature [2, 31], alloys with a high chromium content tend to exhibit a strong interaction between the Cr and N. This effect is typical of conventional stainless steels at a relatively higher temperature, which is characterised by the formation of chromium nitride precipitates [2]. As expected, the surface hardness of the 520 °C plasma nitrided layer is higher than that of the 450 °C plasma nitrided layer due to the more effective precipitation of chromium nitride in the 520 °C plasma nitriding process. In addition, the high surface hardness of the 520 °C plasma nitrided 430 ferritic stainless steel extends through a deeper case. Both precipitation hardening and solution hardening contributed to the higher hardness in the deeper case of the 520 °C plasma nitrided sample [5]. However, the surface hardness of gas nitrided 430 steel sample, which has no obvious and homogeneous nitride layer, is only 310 $HV_{0.01}$.

3.3. Friction coefficient

The results of the friction tests are plotted in graphs showing the friction coefficient against sliding distance for constant load. Friction characteristics obtained for the 450 °C and 520 °C plasma, salt-bath and gas nitrided 430 ferritic stainless steel samples are shown in Fig. 5.

The experimental results showed that the friction characteristics of the nitrided samples significantly depend on the nitriding technique. The friction coefficient of the salt-bath nitrided 430 sample was found to be better than that of the other nitrided samples. In the steady states towards the end of the friction tests, the friction coefficient of the salt-bath nitrided 430 sample was about 0.12, whilst the friction coefficient values of the 450 °C and 520 °C plasma nitrided as well as gas nitrided 430 samples were about 0.45, 0.28 and 0.65, respectively. The results imply that the salt-bath nitrided steel surface reduced the friction to some extent, which can be linked to the change in the surface hardness, microstructure, especially that of the white layer at the top on the nitrided surface, surface roughness and compressive residual stress [4] in the nitrided layer of the 430 steel surfaces after the salt-bath nitriding process. On the other hand, the friction characteristics of the 520 °C plasma nitrided sample, which has the maximum surface hardness and maximum case depth, are better than those of the 450 °C plasma nitrided sample.

It must be pointed out that the friction coefficients of plasma and salt-bath nitrided samples were very uniform during the friction tests. The friction coefficient values of the plasma and salt-bath nitrided samples increased almost linearly with increasing sliding distance. However, the friction coefficient curve of the gas nitrided sample showed a noticeable change in the slope after about 40 m of sliding distance, which could indicate a change in the mechanism involved in the wear process. The gas nitrided samples had no obvious and homogenous nitrided layer, which is an expected result given the high surface roughness of these samples. The highest friction coefficients were found for the gas nitrided 430 ferritic stainless steel samples than the other nitrided samples because the plasma nitrided and salt-bath nitrided samples, which had a much larger surface hardness than the gas nitrided samples, had better resistance to ploughing and adhesion. The micro-images of the worn surfaces of the nitrided samples are shown in Fig. 6. Microscopic surface observations of the worn plasma and salt-bath nitrided samples, especially for the salt-bath nitrided sample with a brittle white layer, showed a fractured nitrided case with exfoliation on the surfaces during friction testing with a constant load (Fig. 6, a, b, c). On the other hand, the worn surface of the gas nitrided sample, which has the highest friction coefficient, was mainly characterised by strong adhesion, plastic deformation and tribo-oxidation [1, 5, 20, 32, 33], whilst the worn surface of the plasma nitrided samples showed slight adhesion, abrasion and tribo-oxidation. The high surface hardness can resist the plastic deformation. Particle removal in the gas nitrided sample is clearly observed in Fig. 6, d, mainly due to adhesion and oxidation mechanisms. No scratches were found in the gas nitrided sample. The stronger adhesive mechanism produced a higher friction coefficient in the 430 nitrided steel samples. On the other hand, the worn surface of the salt-bath nitrided sample showed signs of exfoliation, slight adhesion and tribo-oxidation. No scratches appeared in the salt bath nitrided sample, which could conform to the significantly lower friction coefficient of the salt- bath nitrided 430 ferritic stainless steel samples compared with the other nitrided samples, especially the gas nitrided samples.

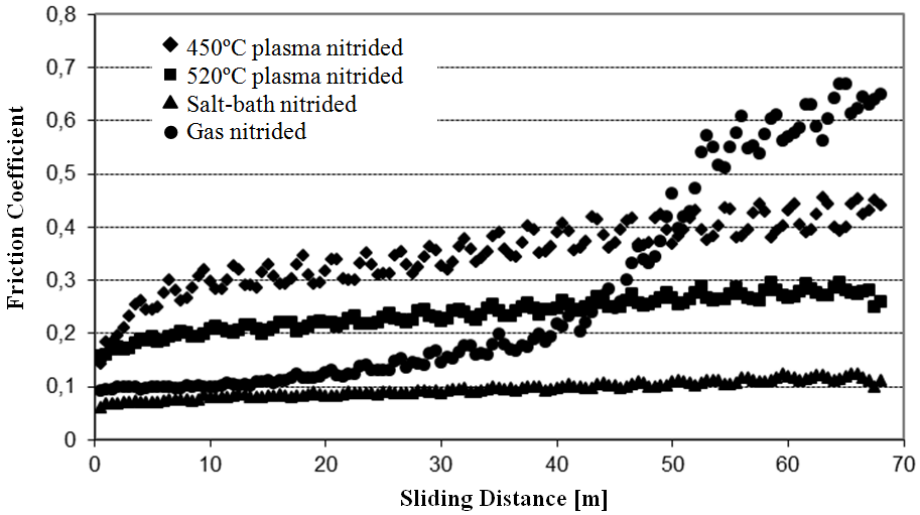

Fig. 5. Friction coefficients of different nitrided 430 ferritic stainless steel samples

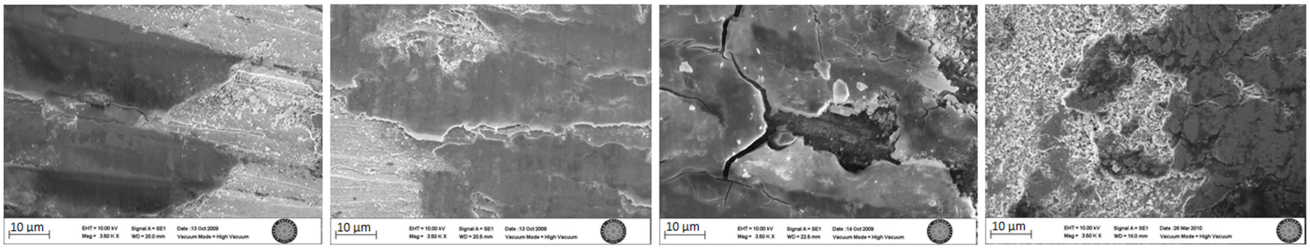

a b c d

Fig. 6. Detail of wear tracks of 450 °C plasma nitrided (a), 520 °C plasma nitrided (b), salt-bath nitrided (c) and gas nitrided (d) 430 ferritic stainless steel samples

4. CONCLUSIONS

In this work, the effect of DC-pulsed plasma nitriding at 450 ºC and 520 ºC, salt-bath nitriding and gas nitriding techniques on the friction coefficient of AISI 430 ferritic stainless steel was investigated using a ball-on-disc friction-wear tester with a WC-Co ball as counter-body under dry sliding conditions. The conclusions derived from this study can be given as follows:

Various nitriding techniques produced different nitride layers in 430 ferritic stainless steels in terms of morphology and thickness. The maximum case depth was achieved on the high temperature plasma nitrided samples at 520 ºC. However, the gas nitriding technique at 570 ºC for 13 h was not sufficient to form a hard nitride layer on the 430 ferritic stainless steel surfaces. The plasma nitrided layers on the 430 steel surfaces consisted of only a nitrogen diffusion layer, whilst the salt-bath nitrided samples had a thin white layer at the top and a nitrogen diffusion layer beneath in the nitride layer.

The plasma and salt-bath nitriding techniques significantly decreased the average surface roughness of the 430 ferritic stainless steel samples. The lowest average surface roughness value was obtained in the 520 ºC plasma nitrided sample, whilst the gas nitriding sample had the highest surface roughness.

The plasma and salt-bath nitriding processes significantly increased the surface hardness. The high temperature (520 ºC) plasma nitrided 430 steel sample had the highest surface hardness with 1490 $HV_{0.01}$. In addition, the high plasma nitriding temperature significantly increased the effective case depth in 430 steel.

The friction characteristics of the nitrided samples depended significantly on the nitriding technique. The salt-bath nitrided 430 ferritic stainless steel samples exhibited much lower friction coefficient values than the plasma nitrided and gas nitrided samples. This can be associated with the effects of the high surface hardness, the morphology of the nitrided layer, especially the white layer formed at the top on the nitrided surface, and the low surface roughness. On the other hand, the friction coefficient of the plasma nitrided sample at 520 °C, which had the maximum surface hardness and maximum case depth, was better than that at 450°C.

REFERENCES

1. **Xia, Y., Hu, J., Zhou, F., Lin, Y., Qiao, Y., Xu, T.** Friction and Wear Behavior of Plasma Nitrided 1Cr18Ni9Ti Austenitic Stainless Steel under Lubrication Condition *Materials Science and Engineering: A* 402 2005: pp. 135 – 141. http://dx.doi.org/10.1016/j.msea.2005.04.012
2. **Pinedo, C. E., Monteiro, W. A.** Surface Hardening by Plasma Nitriding on High Chromium Alloy Steel *Journal of Materials Science Letters* 20 2001: pp. 147 – 149.
3. **Sun, T., Bell, T.** Plasma Surface Engineering of Low Alloy Steel *Materials Science and Engineering: A* 140 1991: pp. 419 – 434.

4. **Xi, Y., Liu, D., Han, D.** Improvement of Corrosion and Wear Resistances of AISI 420 Martensitic Stainless Steel Using Plasma Nitriding at Low Temperature *Surface and Coatings Technology* 202 2008: pp. 2577 – 2583.
5. **Li, C. X., Bell, T.** Sliding Wear Properties of Active Screen Plasma Nitrided 316 Austenitic Stainless Steel *Wear* 256 2004: pp. 1144 – 1156.
6. **Bell, T., Dearnley, P. A.** Environmental Issues in Surface Engineering and Related Industrial Sectors *Surface Engineering* 10 (2) 1994: pp. 123 – 128.
7. **Sun, Y., Bell, T.** Sliding Wear Characteristics of Low Temperature Plasma Nitrided 316 Austenitic Stainless Steel *Wear* 218 1998: pp. 34 – 42.
8. **Blawert, C., Mordike, B. L.** Industrial Applications of Plasma Immersion Ion Implantation *Surface and Coatings Technology* 274 (9) 1993: pp. 274 – 279.
9. **Xu, X., Wang, L., Yu, Z., Qiang, J., Hei, Z.** Study of Microstructure of Low-Temperature Plasma-Nitrided AISI 304 Stainless Steel *Metallurgical and Materials Transactions A* 21A 2000: pp. 1193 – 1199.
10. **Zhang, Z. L., Bell, T.** Structure and Corrosion Resistance of Plasma Nitrided Stainless Steel *Surface Engineering* 1 (2) 1985: pp. 131 – 136.
11. **Samandi, M., Shedden, B. A., Bell, T., Collins, G. A., Hutchings, R., Tendys, J.** Significance of Nitrogen Mass Transfer Mechanism on The Nitriding Behaviour of Austenitic Stainless Steel *Journal of Vacuum Science and Technology B* 12 (2) 1994: pp. 935 – 939.
12. **Menthe, E., Rie, K. T., Schultze, J. W., Simson, S.** Structure and Properties of Plasma-Nitrided Stainless Steel *Surface and Coatings Technology* 74 – 75 1995: pp. 412 – 416.
13. **Kuzucu, V., Aksoy, M., Korkut, M. H.** The Effect of Strong Carbide-Forming Elements such as Mo, Ti, V and Nb on The Microstructure of Ferritic Stainless Steel *Journal of Materials Processing Technology* 82 1998: pp. 165 – 171.
14. **Unterweiser, P. M., Boyer, H. E., Kubbs, J. J.** Heat Treater's Guide: Standard Practices and Procedures for Steel. ASM, Metals Park, 1993.
15. **Kaçar, R., Gündüz, S.** Increasing The Strength of AISI 430 Ferritic Stainless Steel by Static Strain Ageing *Kovove Materialy* 47 2009: pp. 185 – 191.
16. **Sung, J. H., Kong, J. H., Yoo, D. K., On, H. Y., Lee, D. J., Lee, H. W.** Phase Changes of The AISI 430 Ferritic Stainless Steels After High-Temperature Gas Nitriding and Tempering Heat Treatment *Materials Science and Engineering A* 489 2008: pp. 38 – 43.
17. **Rolinski, E.** Effect of Plasma Nitriding Temperature on Surface Properties of Austenitic Stainless Steel *Surface Engineering* 3 1987: pp. 35 – 40.
18. **Mändl, S., Günzel, R., Richter, E., Möller, W.** Nitriding of Austenitic Stainless Steels Using Plasma Immersion Ion Implantation *Surface and Coatings Technology* 100 – 101 1998: pp. 372 – 376.
19. **Sun, Y., Bell, T., Wood, G.** Wear Behaviour of Plasma-Nitrided Martensitic Stainless Steel *Wear* 178 1994: pp. 131 – 138.
20. **Li, G., Peng, Q., Li, C., Wang, Y., Gao, J., Chen, S., Wang, J., Shen, B.** Effect of DC Plasma Nitriding Temperature on Microstructure and Dry-Sliding Wear Properties of 316L Stainless Steel *Surface and Coatings Technology* 202 (12) 2008: pp. 2749 – 2754. http://dx.doi.org/10.1016/j.surfcoat.2007.10.002
21. **Alphonsa, I., Chainani, A., Raole, P. M., Ganguli, B., John, P. I.** A Study of Martensitic Stainless Steel AISI 420 Modified Using Plasma Nitriding *Surface and Coatings Technology* 2 – 3 2002: pp. 263 – 268.
22. **Özdemir, U., Erten, M.** The Effect of Plasma Nitriding on the Material Properties *Havacılık ve Uzay Teknolojileri Dergisi* 1 (2) 2003: pp. 41 – 48 (in Turkish).
23. **Korkmaz, E. E.** Investigation of Microstructure and Mechanical Properties of Cold Work Tool Steels Hardened Surface by Ion Implantation and Plasma Nitriding Method. *PhD Thesis* Uludag University, Bursa, 2009 (in Turkish).
24. Treat All Metals. Nitriding. *http://www.treatallmetals.com/nitrid.htm*, Access date: 13.01.2009.
25. **Zhu, X., Yan, Z., Xu, J.** Ion Penetration and Diffusion Technique at Atmospheric Pressure *Surface and Coatings Technology* 201 2007: pp. 5435 – 5437. http://dx.doi.org/10.1016/j.surfcoat.2006.07.011
26. **Usta, M., Oney, I., Yildiz, M., Akalin, Y., Ucisik, A. H.** Nitriding of AISI 316L Surgical Stainless Steel in Fluidized Bed Reactor *Vacuum* 73 2004: pp. 505 – 510.
27. **Vandendael, I., Steenhaut, O., Hubin, A., Vereecken, J., Prince, P., Reniers, F., Segato, T.** AES Analysis of Nitride Layers on Steel with Target Factor Analysis *Surface and Interface Analysis* 30 2004: pp. 1093 – 1097. http://dx.doi.org/10.1002/sia.1848
28. **Sun, Y., Kolosuary, Z., Flis, J.** The Response of Austenitic Stainless Steels to Low Temperature Plasma Nitriding *Heat Treatment of Metals* 1 1999: pp. 9 – 16.
29. **Marchev, K., Cooper, C. V., Blucher, J. T., Giessen, B. C.** Conditions for The formation of A Martensitic Single-Phase Compound Layer in Ion-Nitrided 316L Austenitic Stainless Steel *Surface and Coatings Technology* 99 1998: pp. 225 – 8. http://dx.doi.org/10.1016/S0257-8972(97)00532-X
30. **Stagno, E., Pinasco, M. R., Ienco, M. G., Palombarini, G., Bocchini, G. F.** Behaviour of Sintered 410 Low Carbon Steels Towards Ion Nitriding *Journal of Alloys and Compounds* 247 1997: pp. 172 – 179. http://dx.doi.org/10.1016/S0925-8388(96)02604-7
31. **Jack, K. H.** Nitriding. Conference on Heat Treatment. The Metals Society, London 1973: pp. 39 – 50.
32. **Corengia, P., Walther, F., Ybarra, G., Sommadossi, S., Corbari, R., Broitman, E.** Friction and Rolling-Sliding Wear of DC-Pulsed Plasma Nitrided AISI 410 Martensitic Stainless Steel *Wear* 260 2006: pp. 479 – 485.
33. **Velasco, F., Martinez, M. A., Calabres, R., Bautista A., Abenojar, J.** Friction of PM Ferritic Stainless Steels at Temperatures up to 300 ºC *Tribology International* 42 2009: pp. 1199 – 1205. http://dx.doi.org/10.1016/j.triboint.2009.04.017